

Interfacial Tension Measured at Nitrogen–Liquid and Liquid–Liquid Interfaces Using Model Microemulsions at High-Pressure and High-Temperature Conditions

Zlata Grenoble and Siwar Trabelsi*



Cite This: <https://doi.org/10.1021/acs.energyfuels.1c01358>



Read Online

ACCESS |



Metrics & More

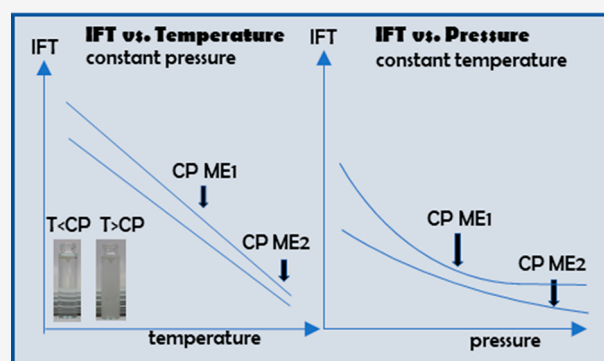


Article Recommendations



Supporting Information

ABSTRACT: The interfacial tensions (IFTs) of two different model microemulsion systems were studied at high-temperature and high-pressure (HTHP) conditions at the nitrogen–brine interface. The experimental scope covers the temperature range 25–100 °C, and a pressure range from atmospheric to 300 bar, more representative of some reservoir conditions. A nonionic ethoxylated alkyl ether based microemulsion (ME1) and a nonionic sugar based microemulsion (ME2) were selected for this study. ME2 was chosen for its tolerance to high salinity and temperature. Favorable interactions between the microemulsions and nitrogen lead to substantial IFT reduction. Low IFT values of 14.36 and 13.1 mN m⁻¹ were measured for ME1 and ME2, respectively, at the highest temperature and pressure settings, far below the IFT value measured for nitrogen–brine with no microemulsion (40.2 mN m⁻¹). Both microemulsions (ME1 and ME2) maintained their IFT lowering capabilities far beyond their respective cloud points. No loss of IFT lowering performance or surfactant phase separation was observed over the studied temperature and pressure ranges. The IFT between 0.2 vol % ME2 and a crude oil was also measured at HTHP conditions. ME2 demonstrated phase stability at the crude oil interface up to 80 °C and retained its IFT lowering performance at even higher temperatures. ME2 reduced interfacial tension at the crude oil–brine interface to values of 0.2–0.5 mN m⁻¹, without any measurable adverse effects of pressure and temperature on the IFT.



1. INTRODUCTION

Microemulsions have several applications in well cleanup (e.g., remediation) and stimulation (e.g., hydraulic fracturing) as well as enhanced oil recovery (EOR) and improved oil recovery (IOR). Capillary pressure represents the pressure required for the hydrocarbon to force water out of the pores of the subterranean formation. Water that remains in the pores near the wellbore forms water blocks that prevent the flow of hydrocarbon into the wellbore. As shown in Rostami et al.'s study, displacement of the hydrophobic hydrocarbon gas phase is, in particular, problematic.^{1,2} Applying microemulsions may lower the capillary pressure between the water and the oil, which increases flowback recovery and hydrocarbon production.³ Frequently, the laboratory experiments described in the literature involved aging tests of the respective treatment fluids at high temperatures. However, the analytical methods, i.e., contact angle and surface tension (SFT) measurements, or core flooding tests, were carried out at ambient conditions. Oil production enhancement by microemulsion addition to fracturing fluids in low-permeability reservoirs was demonstrated by Liang et al.² and Santanna et al.^{3,4} Qin et al. studied microemulsion performance with heterogeneous cores, which were more representative of the mineral composition found in

reservoir rocks.⁵ Javanbakht et al. found that a microemulsion was more efficient than the surfactant alone for wettability alteration and capillary pressure reduction. The authors concluded that a slight decrease in interfacial tension (IFT) relative to the surfactant solutions promoted additional capillary pressure reduction. The primary driving force for wettability alteration and hydrocarbon cluster displacement was the solvent (d-limonene), which promoted surfactant diffusion to the surface and easy penetration of the oil layer.⁶ These studies focused on the relationship between microemulsion efficiency and rock characteristics. They also included effects of brine salinity and varying surfactant–solvent concentrations on wettability alteration and fluid displacement. Their primary tools were core flooding experiments using model cores, with known mineral compositions. Experimental conditions were mostly limited to ambient

Received: May 5, 2021

Revised: July 26, 2021

temperature and pressure. In contrast, reservoir temperature conditions of a carbonate reservoir were simulated in core flooding experiments by Karambeigi et al.⁷ They demonstrated improved crude oil recovery and temperature stability up to 75 °C of a novel microemulsion that contained a fatty acid mixture as the oil phase as compared to conventional water flooding in a carbonate formation. Their study, however, did not include IFT behavior studies at elevated pressures.

One important factor in downhole reservoir applications is the phase stability of the microemulsion system at high-temperature and high-pressure conditions. Surfactant loss due to adsorption to rock surfaces is an additional incentive to develop surfactant/microemulsion systems for specific reservoirs. The phase stability and performance of a microemulsion at HTHP conditions are generally associated with the cloud point of the surfactant. The cloud point is defined as the temperature at which the solution becomes cloudy.⁸ The cloudy appearance arises from phase separation into a micelle-rich solution and a surfactant-depleted, diluted phase. Cloud point behavior is correlated to surfactant structure and properties, and it depresses with increasing brine salinity and temperature. It has been suggested that these cloud point related phase transitions lead to loss of surfactant performance and other adverse effects. The data provide good insight into designing reservoir-compatible treatment fluids and formation damage prevention, they but do not include effects of gases, i.e., nitrogen or CO₂, at high pressures.^{9,10} As demonstrated in section 3, a better understanding of the reservoir condition effects on the cloud point or phase behavior in the presence of gases can help prevent an increase in IFT and potential formation damage due to surfactant phase separation.

Wettability alteration has been assessed by measurements of contact angle, capillary number, and IFT, over a limited range of temperatures and pressures.^{11–14} Imbibition studies on water-wet hydrophilic surfaces suggest lower surfactant concentration requirements for efficient IFT reduction,¹⁵ which appears to be contradictory to observations of surfactant bilayers formed on water-wet hydrophilic surfaces as compared to monolayer formation on oil-wet hydrophobic surfaces.¹⁶ These apparent discrepancies are related to different mechanisms. The surfactant concentrations used in imbibition studies contained high surfactant concentrations, which were far above the critical micelle concentration (cmc). The results did not strictly reflect surfactant loss due to adsorption at the surface and surfactant depletion from the bulk. Adsorption mechanisms and related surfactant–surface interaction on model surfaces were investigated by Karambeigi et al. and Zhang et al.^{7,17} Studies on carbonate surfaces and rocks, carrying positive surface charges, with mostly oil or mixed wet surface properties, demonstrated how appropriate selection of surfactant type, solvent properties, and fluid composition result in enhanced wettability alteration of carbonate reservoirs.^{18–20} Pal et al. presented comprehensive phase behavior data on microemulsion systems containing an anionic temperature- and brine-tolerant methyl ester sulfonate. Their study provides insight into favorable microemulsion phase behavior and stability, with good results in EOR applications.²¹ However, IFT measurements and phase stability for both surfactants and microemulsions have been limited to a narrow temperature and pressure range, not fully representative of HTHP reservoir conditions. One study of nanofluids containing surfactants and zirconia nanoparticles was conducted by Jha et al. at a temperature of 70 °C and an elevated pressure of 20 MPa (200

bar).²² The experimental temperature and pressures might be considered representative for HTHP reservoir conditions, presenting new aspects on the relationship between wettability alteration and concentration levels. The researchers showed that wettability alteration of quartz surfaces was related to cation–anion interactions in low salinity brines and depended on the nanoparticle concentration. The IFT generally decreased when the nanofluid was used at optimum concentrations at the respective temperature and pressure conditions. No information was presented on IFT dynamics with varying temperature and pressure.

Numerous studies have focused on microemulsion and surfactant performance at low temperatures and atmospheric pressure, but to our knowledge, no significant studies are available on the interfacial behaviors, phase stabilities, and cloud point behaviors of surfactants and microemulsions over a wide range of pressure and temperature conditions more representative of some reservoir conditions. The generally prevailing assumptions regarding cloud point effects involve temperature and pressure dependent phase changes and reduced surfactant efficiency.²³ The present study focuses on the IFT behavior of two model microemulsions at high-temperature and -pressure conditions below and above the cloud point, using nitrogen as the second fluid phase and the pressurization medium. The IFT was also measured between one of the model formulations and a crude oil at HTHP conditions.

The IFT was measured using a high-pressure, high-temperature cell, integrated with pendant/rising drop shape analysis. This combined system provides a suitable experimental platform for studying temperature and pressure effects on the interfacial tension of microemulsions at the nitrogen–liquid and liquid–liquid interfaces.

2. MATERIALS AND METHODS

2.1. Materials. Industrial grade nitrogen was used as the pressurization medium at the liquid–liquid interface and as the gas/supercritical fluid phase medium for studies at the nitrogen–liquid interface. Nitrogen was present in its gaseous form at atmospheric pressure and as a supercritical fluid at elevated pressure conditions ($P_c = 33.5$ bar (3.3 MPa), $T_c = -146$ °C (126 K)). Nitrogen was also used as the pressurization medium of liquid–liquid systems. Motivation for using nitrogen as the fluid phase arose from its potential application as an alternative to CO₂ flooding/injection. It is known that CO₂ flooding leads to improved oil recoveries by enhancing IFT reduction at the crude oil–brine interface.^{24–30} However, there are concerns regarding a shift of asphaltene precipitation onset (APO) to lower pressure and temperature.³ Supercritical nitrogen is considered a less hydrophobic fluid and might be an alternative to CO₂, delaying asphaltene precipitation.^{28,31,32}

All solvents, cosolvents, and surfactants were used as supplied by the manufacturers. Ultrapure Milli-Q water (>18.2 MΩ) was used in all experiments.

Two model microemulsion (ME) systems were used in this study, each at a concentration of 0.2 vol %. We have chosen this concentration, since it represents a good average concentration slightly higher than or equivalent to those applied in the field and corresponds to the equivalent unit of 2 gpt (gallons per 1000 gallons).^{2,11,33} The surfactant concentrations within the MEs are typically several times the critical micellar concentration (cmc) for optimum IFT reduction and treatment efficiency, even after surfactant loss due to adsorption to the reservoir rock surfaces.

ME1 consists of 23 wt % nonionic ethoxylated alkyl ether (C_{12–14}EO₇), 23 wt % isopropyl alcohol (IPA), 15 wt % d-limonene, and 39 wt % water. ME1 was diluted to 0.2 wt % in 2% KCl brine.

ME2 consists of 23 wt % alkyl polyglucoside (APG) (DP = 1.5, alkyl chain length C₈–C₁₆), 6 wt % isoamyl alcohol, 10.0 wt % d-limonene, 5.0 wt % C₁₂ methyl ester, and 56 wt % water. ME2 was diluted to 0.2 wt % in high salinity brine (12 wt % NaCl and 4 wt % CaCl₂). Upon dilution in the aqueous phase, these MEs form solvent swollen micelles.

The cloud points of both ME1 and ME2 were measured in rising drop configuration, using 0.2 vol % dilutions of the microemulsions in the respective brines as the bulk phase (2% KCl brine for ME1 and high salinity brine for ME2). The phase behavior of each system could be monitored as a function of temperature and pressure, and the cloud point was determined by loss of contrast between nitrogen and the brine phase, due to increasing solution turbidity. The cloud point of ME1 was determined at 40 °C, and for ME2, a significantly higher temperature of 80 °C was recorded.

The crude oil used in this study originated from the Permian basin in West Texas (°API = 36.2). SARA analysis showed that the crude oil contained 40.2 wt % saturates, 44.9 wt % aromatics, 14.7 wt % resins, and 0.2 wt % asphaltenes.

2.2. Methods. A Tecnis high-temperature–high-pressure tensiometer was used in this study to measure the IFT at HTHP conditions. The upper temperature and pressure limits were kept at 100 °C and 300 bar. Downhole temperatures and pressures might exceed these values, but our experimental temperature and pressure ranges fall well within the range of HTHP conditions, and the resulting information gained from this study provides new insight into the phase behaviors and stabilities of the microemulsions at high-temperature and high-pressure conditions.^{10,33,43–50} These temperature and pressure limits further ensured that the experimental work was carried out within the safe operation window of the instrument. The Tecnis HTHP tensiometer is controlled via the data acquisition and control software WDROP THP_V8. It combines pendant drop tensiometry (axisymmetric drop shape analysis (ADSA)) with an HTHP cell for experimental studies and measurements of the IFT and the viscoelastic modulus at HTHP conditions (Figure 1). The HTHP



Figure 1. Front image of the HTHP tensiometer.

cell design enables the software-controlled pressurization of the measuring chamber via an air driven compressor pump, integrated into the nitrogen gas supply line. Cell temperature is regulated by a thermostatic circulating bath (Julabo, model Presto A30, Julabo GmbH, Germany).

The cell design allows measurement of the interfacial tension at gas–liquid interfaces in two configurations. In pendant drop configuration, the lower density bulk phase is usually a gas and the internal higher density phase is a liquid, which could be an aqueous or a hydrocarbon phase. The rising drop configuration is suitable for both liquid–gas/fluid and liquid–liquid phase studies. In this case, the internal phase (bubble or drop) was the nitrogen gas/supercritical fluid, surrounded by the diluted ME solution.

The drop shape is recorded by a CCD camera (see Figure 2), followed by drop shape analysis using the software-controlled

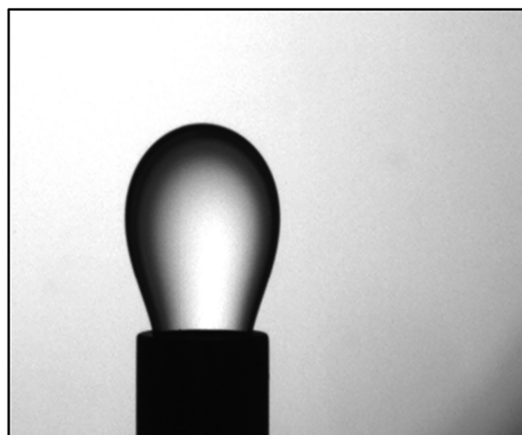


Figure 2. Example of a rising drop configuration: hexadecane drop in water.

algorithm. The image measurement rate (frame rate) is usually set at 1 s⁻¹, or to higher sampling rate of 6 s⁻¹ for oscillatory drop area variations. Requirements for this technique are optical contrast, which depends on refractive index differences between the bulk and drop phases, and the transparency of the bulk phase. Pressure and temperature dependent density corrections for the nitrogen fluid phase were based on empirical equations. The densities of the aqueous phase and the crude oil were derived from physical measurements of densities as a function of temperature at atmospheric pressures. The applied density corrections for nitrogen and water at the respective experimental conditions were validated against literature data (details can be found in the Supporting Information). The measured densities (Anton Paar densitometer, DMA 4500M, Austria) of water up to 55 °C were consistent with theoretical density–temperature curves of water, and they were used for a second order polynomial curve fit. Crude oil densities were measured over the temperature range 25–65 °C and were also fitted to a second order polynomial model. Pressure-corrected densities of water were based on theoretical data, and small density changes of crude oil as a function of pressure were considered. However, based on literature data from reservoir modeling of live and dead crude oils, NIST guidelines, and algorithm checks, pressure effects on the density of dead oil are negligible within the experimental pressure range from atmospheric to 300 bar pressure.^{34,35} The compressibility coefficients of dead oil almost cancel against the expansion coefficients, over the studied temperature and pressure ranges. The applied small density corrections were verified by comparing them to the output from simulator models and literature sources, related to reservoir modeling and phase modeling of both pure hydrocarbons and hydrocarbon mixtures.^{36–43} Test calculations using applied densities versus densities with maximum feasible deviations confirmed that minor deviations of the applied densities are insignificant in the final calculation of SFT/IFT.

3. RESULTS

3.1. ME1: IFT at the Nitrogen–Liquid Interface. The preferred experimental design for this system was the pendant drop configuration. It allows preservation of good contrast between the drop and the bulk phase throughout the experimental sequence, independently of the phase behavior of the diluted ME1.

3.1.1. Equilibrium IFT of ME1 at the Nitrogen–Liquid Interface. The equilibrium IFT between the nitrogen and 0.2 vol % ME1, at different pressure and temperature settings, are

shown in Figure 3. At an atmospheric pressure of 1 bar and 25 °C, the IFT was equal to 28.30 mN m⁻¹ and decreased to the

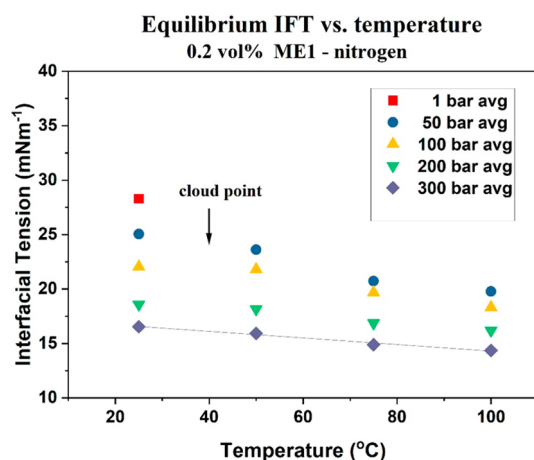


Figure 3. IFT trends of 0.2 vol % ME1 versus temperature at four pressure settings. The cloud point of ME1 (40 °C) is indicated by an arrow.

lowest value of 14.36 mN m⁻¹ at 300 bar and 100 °C. The dominating effects of pressure on IFT reduction are evident from the progressively decreasing slopes or coefficients of $d\gamma/dT$ at isobaric conditions of 50, 100, 200, and 300 bar. The IFT decreases practically linearly with temperature, when the pressure is raised above atmospheric pressure, with a slope of $d\gamma/dT$ of -0.075 at 50 bar and a slope of $d\gamma/dT$ of -0.030 at 300 bar. The IFT versus pressure correlation models, in contrast, show nonlinear trends, with a good fit to a second polynomial model but only small quadratic terms.

At high pressures, $d\gamma/dT$ approaches zero and the IFT becomes practically independent of temperature. The slope of $d\gamma/dP$ at 75 °C is -0.0297 , almost identical to the $d\gamma/dP$ of -0.0305 at 100 °C, and further IFT reduction with higher pressures would be small (Table 1). Only one data point was

Table 1. Fitting Parameters of the IFT Model for the ME1–Nitrogen System

| | pressure | | | |
|---------------------|-------------|-----------|-----------|-----------|
| | 50 bar | 100 bar | 200 bar | 300 bar |
| slope $-d\gamma/dT$ | -0.0749 | -0.0530 | -0.034 | -0.0302 |
| intercept | 26.98 | 23.78 | 19.58 | 17.32 |
| R^2 | 0.969 | 0.962 | 0.972 | 0.985 |
| | temperature | | | |
| | 25 °C | 50 °C | 75 °C | 100 °C |
| slope $-d\gamma/dP$ | -0.0709 | -0.0487 | -0.0297 | -0.0305 |
| intercept | 28.31 | 26.01 | 22.29 | 21.20 |
| R^2 | 0.999 | 0.999 | 0.997 | 0.999 |

acquired at atmospheric pressure (1 bar). As shown in Figure 3 and Table 1, the IFT continuously decreased with increasing temperature for the measured temperatures up to 100 °C. No discontinuity in IFT curves could be observed across the temperature region below and above the cloud point of ME1, which was determined to be equal to 40 °C. ME1 retains its interfacial activity far beyond the cloud point, at least up to 300 bar.

Surface excess was not specifically determined in this study, with a focus on the HTHP stability and performance of microemulsions. Adsorption isotherms would also require a different analytical technique, i.e., the depletion method, to determine the surface excess in micromoles or micrograms per square meter, or computation from the slopes of adsorption isotherms. This process would be more complex at elevated temperatures and pressures, and it would actually not contribute to the objective of this study.

The interfacial regions of nitrogen–gas or nitrogen–liquid at high temperatures and pressures do not compare to typical interfaces encountered at ambient conditions, which have a narrow, constant, and measurable thickness. According to simulations and existing studies,⁵⁴ these regions vary in properties and thickness with the type of gas, temperature, and, in particular, pressure. The mixtures of interacting/mixing surfactants and solvents accumulated in this region may not follow conventional surface excess behavior.

3.1.2. Dynamic IFT of ME1 at the Nitrogen–Liquid Interface. Figure 4 shows the dynamic IFT at 75 °C and

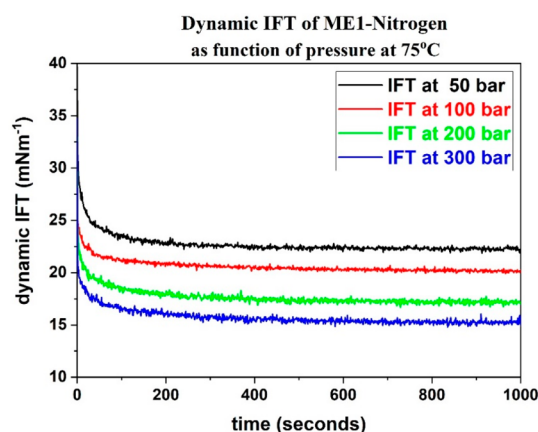


Figure 4. Dynamic IFT of 0.2 vol % ME1 at 75 °C and different pressure settings (50, 100, 200, and 300 bar).

pressure ranging from 50 to 300 bar. The dynamic IFT of ME1 during the initial fluid contact time indicates a fast equilibration time of approximately 150 s, with an exponential decrease of the IFT. These phenomena suggest fast diffusion of solvent and surfactant molecules to the interfacial region. Increasing the pressure did not affect the dynamics of IFT lowering.

3.2. IFT at the Nitrogen–Water Interface. The phase behavior of water–nitrogen as a model system was studied to validate the $\Delta\rho$ values applied for the respective experimental conditions and to demonstrate the effects of nitrogen as a supercritical fluid on IFT at the nitrogen–liquid interface. The experimental scope included IFT measurements at the highest temperature condition of this study, 100 °C, where potential deviations from literature and theoretical values are expected to be most significant, and pressures of 50, 100, 200, and 300 bar. The measured IFT of 40.22 mN m⁻¹ at 100 °C and 300 bar is in agreement with modeled and experimental data.²⁶ Our equilibrium IFT values slightly diverge from the values reported by Chow et al.²⁶ The small deviation of our equilibrium IFT values might be related to equilibration time effects, which are not accounted for in the model (more details are provided in the Supporting Information).

3.3. ME2: IFT at the Nitrogen–Liquid Interface in Rising Drop Configuration. We chose the rising drop configuration to study ME2, where the diluted ME2 is the bulk phase and nitrogen is present in the drop. The rising drop term is used for this configuration, since nitrogen is in its supercritical fluid state and not a gas above the critical pressure of 33.5 bar. One incentive for using a different setup was to allow for visual monitoring of the phase behavior and cloud point identification at different pressure settings. A separate study, conducted in both pendant drop and rising drop configurations, demonstrated that the two configurations are comparable, if surfactant depletion from the bulk and external interferences can be excluded (more information is provided in the [Supporting Information](#)). The rising drop configuration, with the drop in confined space (surrounded by a large supply of solvent molecules from the bulk phase) is more suitable to detect phase behavior changes and measure the cloud point, indicated by increasing solution turbidity and subsequent loss of contrast between the two phases.

3.3.1. Equilibrium IFT of ME2 at the Nitrogen–Liquid Interface. Figure 5 shows the IFT between 0.2 vol % ME2 as a

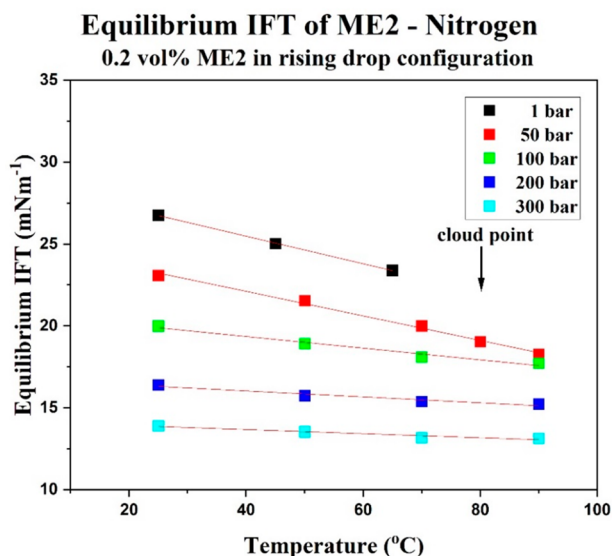


Figure 5. IFT of 0.2 vol % ME2 as a function of temperature, at five different pressure settings of 1, 50, 100, 200, and 300 bar. The cloud point of ME2 (80 °C) is indicated by an arrow.

function of temperature for a set of pressures ranging from 1 to 300 bar. The alkyl polyglucoside contained within ME2 has a higher temperature and salinity tolerance compared to the ethoxylated alkyl ether contained within ME1. As indicated in [section 2](#), the cloud point of ME2 was determined to be equal to 80 °C. The lowest IFT value of 13.1 mN m⁻¹ lies below the lowest IFT of the ME1 system of 14.36 mN m⁻¹. Above 80 °C, phase changes occurred gradually, with measurements feasible up to 90 °C and no performance loss. The cloud point did not change with increasing pressure, and no pressure induced phase separation occurred over the experimental pressure range from atmospheric pressure up to 300 bar.

Figure 6a shows that the IFT–pressure correlations are similar in trend for ME1 and ME2 but vary in magnitude. Up to 50 bar, both systems are practically identical. The nonlinear sigmoidal model gives a good fit to the correlation for the slope of $d\gamma/dT$ at a given pressure. It clearly emphasizes initially

strong temperature effects, which approach a threshold with increasing pressure. At 300 bar, the slope of $d\gamma/dT$ of -0.0124 mN m⁻¹/°C for ME2 is smaller than the slope of -0.0302 mN m⁻¹ for ME1. Both ME1 and ME2 approach the limiting pressure, at which $d\gamma/dT \rightarrow 0$, and temperature does not affect IFT anymore. The APG based formulation ME2 exhibits a lower response to temperature changes but increased response to pressure effects. Both ME1 and ME2 maintain IFT lowering well above their cloud points, with no discontinuity at the cloud point. The trends of $d\gamma/dP$ in [Figure 6b](#) further support the assumption that ME1 is close to its lowest achievable IFT value, whereas ME2 still has a potential for decreasing IFT with increasing pressure. These trends are summarized in [Table 2](#).

3.4. IFT: Rising Drop versus Pendant Drop Configuration. The effects of pendant drop and rising drop geometries were studied using 0.2 vol % ME2. This formulation was chosen for its good temperature stability and high cloud point to study the phase behavior and the IFT using both configurations. The test parameters were 25 °C at 1 bar and 25 and 75 °C at 200 bar in the pendant drop configuration and the rising drop configuration (nitrogen drop/bubble in the 0.2 vol % ME2 aqueous brine phase). These two configurations are expected to provide identical results if surfactant depletion effects or similar interferences are not present. In this case, solvent effects might appear in the rising drop which will not be detectable in the pendant drop configuration. The ratio of gas or supercritical phase volume (100 cm³) in the pendant drop configuration and the liquid volume of the pendant drop (2–5 μL) is large and conducive to solvent evaporation at a fast rate, preventing the detection of solvent effects. This evaporation rate is minimized in the rising drop geometry, where the drop represents the nitrogen volume (also 2–5 μL) versus a liquid volume of 25 cm³.

As shown in [Figure 7](#), the IFT is equal to 27.52 mN m⁻¹ with the pendant drop geometry and 26.42 mN m⁻¹ in the rising drop geometry. Slightly lower IFT values in the rising drop configuration were observed at 25 °C and 200 bar, manifesting as time delayed IFT reduction in the dynamic IFT process. The dynamic IFT exhibits a larger noise at the baseline, and slightly higher IFT values, as compared to the dynamic IFT using the rising drop mode, taken at identical experimental conditions. The IFT measured at 25 °C and 200 bar (black dashed line, rising drop) exhibits an instantaneous IFT decrease at 250 s, related to solvent–nitrogen interactions at elevated pressures.

3.5. Comparative Study of Nitrogen–Crude Oil Interaction. Literature studies of IFT behavior at the interface of nitrogen–hydrocarbon mixtures report substantial IFT reduction, due to nitrogen interaction with crude oils. These IFT lowering trends are opposite to the IFT behavior in the water–hydrocarbon/alkane systems, reported in the literature for brine–hydrocarbon systems in the absence of gases or supercritical fluids,^{43,44} indicating increasing IFT with increasing pressure in water–hydrocarbon/alkane systems, due to the lack of miscibility. In this case, the interaction and miscibility of the fluids with nitrogen molecules favor IFT reduction with increasing pressure and simultaneously decreasing $\Delta\rho$. This IFT–pressure relationship was observed throughout the experiments with nitrogen as the gas or supercritical fluid phase, and it is consistent with related studies.²⁸ Temperature-dependent IFT reduction apparently varies with the systems studied and with the respective models.

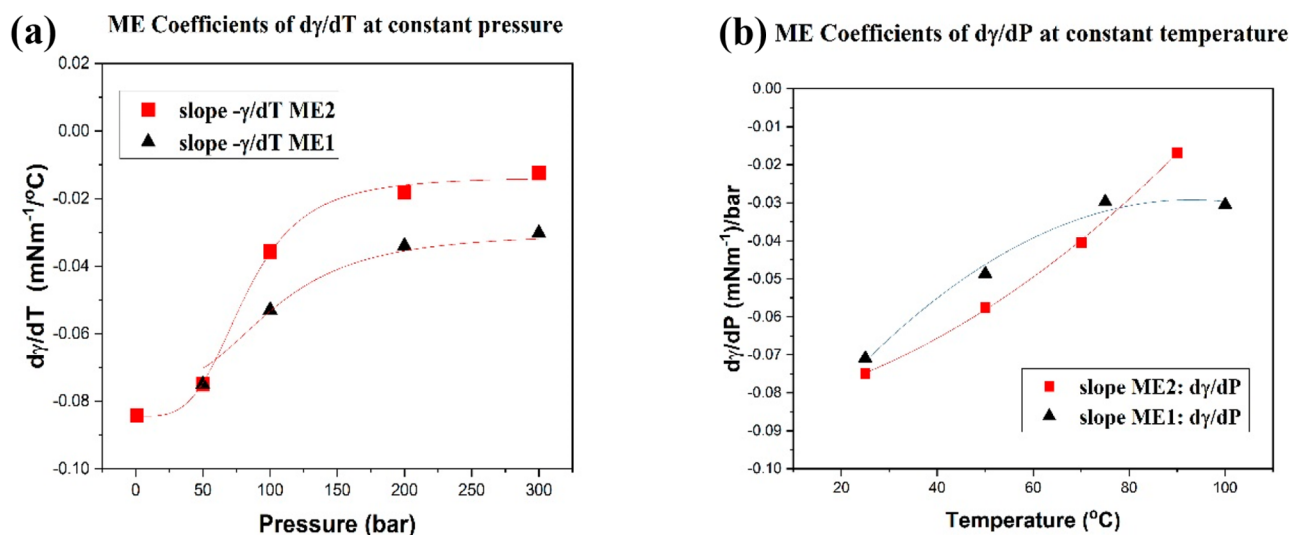


Figure 6. (a) Coefficients of dy/dT for ME1 and ME2 at constant pressure—fitted to a sigmoidal logistic function. (b) Coefficients of dy/dP at constant temperature—fitted to a second order polynomial.

Table 2. Fitting Parameters for the IFT Model and Fit of ME2–Nitrogen System

| | pressure | | | | |
|----------------|-------------|---------|---------|---------|---------|
| | 1 bar | 50 bar | 100 bar | 200 bar | 300 bar |
| slope $-dy/dT$ | -0.0842 | -0.0749 | -0.0356 | -0.0181 | -0.0124 |
| intercept | 28.84 | 25.20 | 20.78 | 16.75 | 14.16 |
| R^2 | 0.9997 | 0.9938 | 0.9761 | 0.9487 | 0.9371 |
| | temperature | | | | |
| | 25 °C | 50 °C | 70 °C | 90 °C | |
| slope $-dy/dP$ | -0.0749 | -0.0576 | -0.0404 | -0.0168 | |
| intercept | 26.67 | 24.13 | 21.86 | 19.27 | |
| R^2 | 0.9976 | 0.9981 | 0.9992 | 0.9930 | |

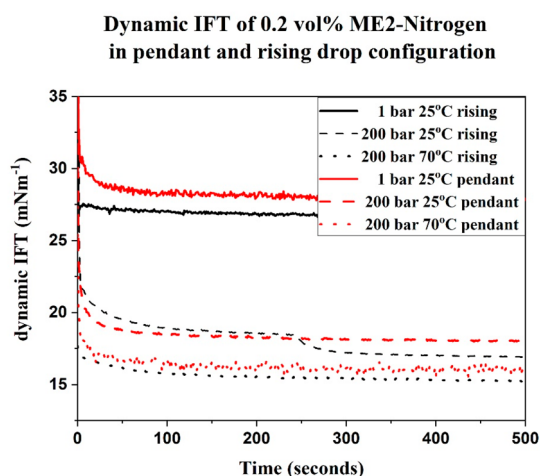


Figure 7. Dynamic IFT for pendant drop and rising drop configurations at different temperature and pressure settings.

The IFTs between nitrogen and the crude oil determined at temperatures from 25 to 90 °C and pressures from 100 to 300 bar lie within the range of literature-reported values for similar crude oils. Hemmati-Sarapardeh et al. measured an IFT of ~ 19 mN m^{-1} at 96 bar and 333 K.²⁹ Our study of the crude oil–water IFT showed an equilibrium IFT value of 18.15 mN m^{-1}

at comparable conditions of 100 bar and 60 °C (graph and more details are provided in the [Supporting Information](#)).

3.6. IFT: ME2 at the Aqueous–Crude Oil Interface. Figure 8 shows the measured IFT between crude oil–water

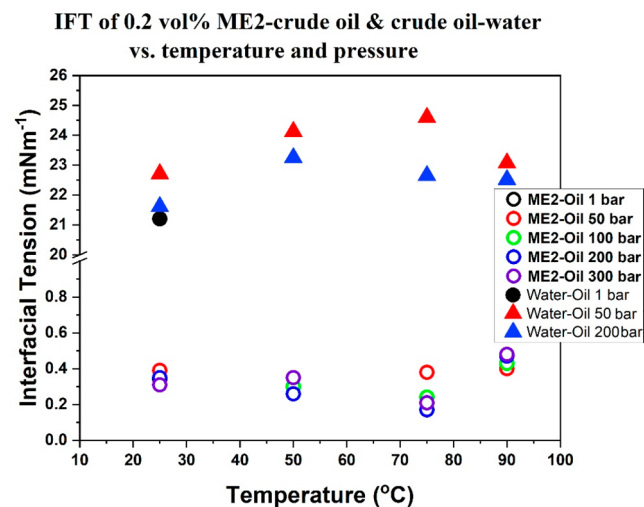


Figure 8. IFT between 0.2 vol % ME2 and crude oil as a function of temperature at different pressure settings. The IFT of crude oil–water is shown as a reference.

and crude oil–ME2 diluted in high salinity brine as a function of temperature for a range of pressure settings. Figure 8 includes only one data point at 1 bar and 25 °C, due to temperature-induced unstable readings of the drop shape. A small IFT increase was observed for the crude oil–water system with increasing pressure to 50 bar, followed by an IFT decrease at 200 bar, independent of the temperature. This pressure-induced IFT decrease might be partly related to increasing fluid compressibility.²³ In this system, combined effects of temperature and pressure are likely to affect the thermodynamics of phase behavior, leading to different arrangements at the water–crude oil interface. The IFT reached its maximum around 75 °C, followed by a decreasing IFT trend. A likely mechanism is an energetically more favorable interaction of water molecules with specific hydro-

carbons once a certain temperature threshold is reached. Figure 8 further illustrates the IFT lowering effects of 0.2 vol % ME2 diluted in high salinity brine. The IFT decreased at any temperature and pressure condition by more than 20 mN m^{-1} , relative to the water–crude oil IFT, which is substantially lower than the IFT induced by the nitrogen alone or the IFT at the nitrogen–water interface (details can be found in the Supporting Information). The IFT values fluctuate between 0.2 and 0.5 mN m^{-1} and decrease slightly with temperature. A small temperature-related IFT reduction was observed up to $75 \text{ }^\circ\text{C}$.

A related HTHP study by Barati-Harooni et al. investigated the effects of temperature, pressure, and different brine salinities on the interfacial tension (IFT) of two live crude oils originating from carbonate oil reservoirs.⁴⁵ Their work included IFT trends at four temperature settings between 315.5 and 373.15 K (40 and $100 \text{ }^\circ\text{C}$), brine salinities from 10 000 to 26 000 ppm, and pressures ranging from 1.38 MPa (13.8 bar; 200 psi) to 34.47 MPa (348 bar; 5000 psi). Their results showed that, for one crude oil, increasing temperature, pressure, and brine salinity of the formation brine increased the IFT value. For the second crude oil, the IFT increased with pressure and salinity but decreased with increasing temperature. The different responses of the two crude oils are related to lower asphaltene content of the former crude oil and different light/heavy fraction ratios, as indicated in their crude oil analysis. Another important factor between their study and our work is the pressurization medium. Barati-Harooni et al.'s study used mechanical pressurization of two immiscible fluids: crude oil and brine. This condition is expected to result in increased fluid densities, a potential increase in salinity, and increased surface energy, as suggested in other studies.²³ A study by Wang et al. expanded the experimental scope over a wide temperature range up to $160 \text{ }^\circ\text{C}$ while maintaining pressure at 50 bar, sufficient to prevent evaporation of the aqueous phase.³³ They did not use any surfactants, but focused primarily on the IFT and interfacial stabilizing effects of various asphaltene and resin weight fractions contained within the model oils. They generally observed decreasing IFTs with increasing asphaltene weight fraction, irrespective of the temperature. This IFT decrease was attributed to different surface activities of the different weight fractions in the model oils. The viscoelastic modulus and interfacial film rigidity increased with increasing temperature and asphaltene concentrations, indicating stabilization of asphaltenic aggregates by asphaltene–resin interactions.

In the present study, nitrogen was used as the pressurization medium. Its favorable interaction with both crude oil and brine fluids^{29,46} leads to lowering of surface energy and significant IFT reduction.²⁸ It also supports the findings that pressure is the dominant parameter affecting IFT reduction, as compared to Barati-Harooni et al.'s⁴⁵ observation that temperature was the most significant contributor. Thermodynamically driven liquid–liquid interaction mechanisms differ from nitrogen–liquid interactions. A general trend has been increasing or invariant IFT with temperature at liquid–liquid interfaces. The microemulsion performance manifests as a substantial IFT reduction without performance loss over the studied temperature and pressure ranges.

4. DISCUSSION

The findings from the study of ME1 and ME2 at the nitrogen gas/supercritical fluid interface confirm the general trends of

cloud point behavior for the nonionic EO and sugar based surfactants. Onset of phase changes is observed at a relatively low temperature of $40 \text{ }^\circ\text{C}$ for ME1, containing the temperature-sensitive nonionic surfactant.⁹ The high-temperature stability and salinity tolerance of ME2 is consistent with previous phase behavior studies of APG-containing microemulsions and characteristic for sugar based surfactants.⁴⁷ For both ME1 and ME2, no performance loss was observed above the cloud point. Both microemulsions maintain phase stability at HTHP conditions and exhibit IFT lowering capabilities. This phenomenon is contrary to previous studies predicting IFT increase at reservoir temperatures above the surfactant cloud point, further accelerated by high salinity brines or the presence of divalent ions.^{10,52} The primary mechanisms for IFT reduction at HTHP conditions in our study are increasing interactions between nitrogen and the liquid phase with increasing nitrogen pressure and decreasing $\Delta\rho$ between the two fluids. Favorable solvent effects improve the interfacial stability in the dynamic process and show a slight reduction of the equilibrium IFT. The slopes of dy/dT and dy/dP (Figure 8) are indicative that ME1 is either close to or has reached the limits of its IFT lowering domain. ME2 still has potential for further IFT reduction with increasing pressure, which makes this system more attractive for high pressure reservoir applications.

A different situation is encountered during the liquid–liquid phase study of ME2–crude oil. The cloud point was observed at $80 \text{ }^\circ\text{C}$, with a slow onset of phase changes, which allowed for IFT measurements beyond the observed cloud point. No surfactant performance decline was observed. Direct nitrogen–liquid interactions are absent at the interface of crude oil and brine containing 0.2 vol % ME2. The solvent contributions are significant for this system, manifested in the improved phase stability and high cloud point of ME2. Increasing pressures did not impact its phase behavior, contrary to expected phase changes reported from related studies.⁴⁹ However, it has also been reported that the solubilization capacities of certain surfactants did not deteriorate at temperatures several degrees above the determined cloud points.⁵¹

Literature data and studies on adverse effects of temperature and pressure on the phase behaviors of surfactants and microemulsions apply to some extent at the liquid–liquid phase. The observed temperature and pressure responses are proportional to the intrinsic structure–property features of the two different surfactant systems, and the selected solvents and cosolvents.²³ This is evident from a comparison of the cloud points of ME1 with ME2. The higher cloud point of ME2 allows maintenance of the phase stability and favorable interactions with nitrogen, and crude oil as the liquid phase, over a wider temperature range.

It is difficult (if at all possible) to provide a direct visual or direct imaging of the increased nitrogen density with the current technique, but we refer to related literature studies which indicate the interfacial thickness modulation as function of mixing media (gases, liquids), and conditions.^{53,54} A method for nitrogen density assessment has been described in the literature, the synthetic visual method,⁵³ and was used as an additional reference for and validation of the theoretically determined nitrogen densities in our study. Temperature and pressure measurements and controls are integral parts of the instrument and used for setting and monitoring the temperature and pressure conditions in the measuring cell. The density changes of N_2 were determined as outlined in section

2.2 and verified by comparison with literature data, as described in more detail in the [Supporting Information](#). The nitrogen density changes and, consequently, $\Delta\rho$ changes between internal and external phases with temperature and pressure are continuously fed into the software calculation algorithm, which updates the nitrogen density value continuously and applies it to the surface tension measurement for each collected data point. Increasing nitrogen density leads to declining $\Delta\rho$ between nitrogen and the second phase, i.e., aqueous phase with ME2 or crude oil, leading to reduced IFT. We could verify this process by monitoring the data acquisition and checking each raw data file. What is significant for IFT reduction at the N_2 –water phase versus the N_2 –aqueous phase with ME are the second IFT lowering mechanisms: IFT decreases as a function of favorable interactions of surfactant–solvent–nitrogen, leading to additive IFT reducing effects.

We also demonstrated the stabilities and efficiencies of MEs at HTHP conditions and confirmed the dominance of pressure over temperature. Our findings suggest that increasing nitrogen pressure, and thus higher nitrogen density, combined with its interaction with suitable surfactant–solvent systems, has additive effects on IFT reduction.

5. CONCLUSION

Our study demonstrates the IFT reducing capabilities of two model formulations at nitrogen–liquid and liquid–liquid interfaces at HTHP conditions. The experimental design and calculation algorithms were validated against reference systems and published literature data. Both ME1 and ME2 significantly reduce the IFT at the nitrogen–liquid interface, with no performance loss at HTHP conditions. Each retains its performance at high-temperature and high-pressure reservoir conditions, and both remain effective at temperatures above their cloud points. None of the microemulsions is negatively affected by increasing pressures up to 300 bar. As the correlations of $d\gamma/dT$ and $d\gamma/dP$ indicate, ME2 has the potential for IFT reduction with further increasing pressure.

IFT reduction by ME2 is substantial at the liquid–liquid interface (crude oil–brine) but relatively invariant across the temperature and pressure ranges studied. Favorable nitrogen interaction with the liquid phase is one of the mechanisms driving the IFT lowering trends in nitrogen–liquid (crude oil) systems. Pressure effects are more significant than temperature-induced interfacial modulation. Solvent effects can be significant, as observed in the phase stabilizing properties of the solvent in ME2. Phase behavior and phase changes are primarily temperature related and are not affected by pressure. The most relevant findings of this study are the phase stability of ME2 at high temperatures. Remarkable is the observation that no loss of interfacial activity is observed at high-pressure conditions up to 300 bar and temperatures above the ME2 cloud point. Future studies with different systems may provide more insight on interaction mechanisms of gas/supercritical fluid–liquid and gas–surfactant–solvent systems and their effects on interfacial properties.

■ ASSOCIATED CONTENT

SI Supporting Information

The Supporting Information is available free of charge at <https://pubs.acs.org/doi/10.1021/acs.energyfuels.1c01358>.

Validation of calculation algorithm for nitrogen–water density corrections; comparison of pendant and rising

drop configurations; IFT behavior at the nitrogen–water interface ([PDF](#))

■ AUTHOR INFORMATION

Corresponding Author

Siwar Trabelsi – Global Research Innovation Center, Flotek Chemistry, Houston, Texas 77064, United States; orcid.org/0000-0003-0866-6539; Email: strabelsi@flotekind.com

Author

Zlata Grenoble – Global Research Innovation Center, Flotek Chemistry, Houston, Texas 77064, United States; Present Address: Spring, TX 77389, USA; Author: Please review the change made to the present address for Z.G. and include any further changes in your list of proof corrections

Complete contact information is available at: <https://pubs.acs.org/10.1021/acs.energyfuels.1c01358>

Notes

The authors declare no competing financial interest.

■ REFERENCES

- (1) Rostami, A.; Nasr-El-Din, H. A. Microemulsion vs. Surfactant Assisted Gas Recovery in Low Permeability Formations with Water Blockage. *SPE Western North American and Rocky Mountain Joint Meeting*; Society of Petroleum Engineers: 2014. DOI: [10.2118/169582-MS](https://doi.org/10.2118/169582-MS).
- (2) Liang, T.; Li, Q.; Liang, X.; Yao, E.; Wang, Y.; Li, Y.; Chen, M.; Zhou, F.; Lu, J. Evaluation of Liquid Nanofluid as Fracturing Fluid Additive on Enhanced Oil Recovery from Low-Permeability Reservoirs. *J. Pet. Sci. Eng.* **2018**, *168*, 390–399.
- (3) Kharghoria, A.; Lett, N.; Portwood, J. T.; Biswas, D.; Hammond, C.; Penny, G.; Rigoris, A. Laboratory to Field Scale Simulation of a Complex Micro-Emulsion System Performance for Enhanced Oil Recovery. *SPE Asia Pacific Enhanced Oil Recovery Conference, EORC 2015*; Society of Petroleum Engineers: 2015; pp 1127–1144.
- (4) Santanna, V. C.; Silva, A. C. M.; Lopes, H. M.; Sampaio Neto, F. A. Microemulsion Flow in Porous Medium for Enhanced Oil Recovery. *J. Pet. Sci. Eng.* **2013**, *105*, 116–120.
- (5) Qin, T.; Javanbakht, G.; Goual, L.; Piri, M.; Towler, B. Microemulsion-Enhanced Displacement of Oil in Porous Media Containing Carbonate Cements. *Colloids Surf., A* **2017**, *530* (July), 60–71.
- (6) Javanbakht, G.; Arshadi, M.; Qin, T.; Goual, L. Micro-Scale Displacement of NAPL by Surfactant and Microemulsion in Heterogeneous Porous Media. *Adv. Water Resour.* **2017**, *105*, 173–187.
- (7) Karambeigi, M. S.; Nasiri, M.; Haghghi Asl, A.; Emadi, M. A. Enhanced Oil Recovery in High Temperature Carbonates Using Microemulsions Formulated with a New Hydrophobic Component. *J. Ind. Eng. Chem.* **2016**, *39*, 136–148.
- (8) Lindman, B.; Medronho, B.; Karlström, G. Clouding of Nonionic Surfactants. *Curr. Opin. Colloid Interface Sci.* **2016**, *22*, 23–29.
- (9) Jachnik, R. P.; Green, P. Horizontal Well Drill-In Fluid Utilising Alcohol Ethoxylate. *SPE International Symposium on Oilfield Chemistry*; Society of Petroleum Engineers: 1995. DOI: [10.2118/28963-MS](https://doi.org/10.2118/28963-MS).
- (10) Nasr-El-Din, H. A.; Al-Ghamdi, A. M. Effect of Acids and Stimulation Additives on the Cloud Point of Nonionic Surfactants. *SPE Formation Damage Control Symposium*; Society of Petroleum Engineers: 1996; pp 397–416. DOI: [10.2118/31106-MS](https://doi.org/10.2118/31106-MS).

- (11) Alvarez, J. O.; Saputra, I. W. R.; Schechter, D. S. Potential of Improving Oil Recovery with Surfactant Additives to Completion Fluids for the Bakken. *Energy Fuels* **2017**, *31* (6), 5982–5994.
- (12) Pal, N.; Vajpayee, M.; Mandal, A. Cationic/Nonionic Mixed Surfactants as Enhanced Oil Recovery Fluids: Influence of Mixed Micellization and Polymer Association on Interfacial, Rheological, and Rock-Wetting Characteristics. *Energy Fuels* **2019**, *33*, 6048–6059.
- (13) Kumar, S.; Panigrahi, P.; Saw, R. K.; Mandal, A. Interfacial Interaction of Cationic Surfactants and Its Effect on Wettability Alteration of Oil-Wet Carbonate Rock. *Energy Fuels* **2016**, *30* (4), 2846–2857.
- (14) Saputra, I. W. R.; Park, K. H.; Zhang, F.; Adel, I. A.; Schechter, D. S. Surfactant-Assisted Spontaneous Imbibition to Improve Oil Recovery on the Eagle Ford and Wolfcamp Shale Oil Reservoir: Laboratory to Field Analysis. *Energy Fuels* **2019**, *33*, 6904–6920.
- (15) Zelenev, A. S.; Grenoble, Z. Wettability of Reservoir Rocks Having Different Polarity by a Model Nonionic Surfactant: Fluid Imbibition Study into Crushed Rock Packs. *Energy Fuels* **2018**, *32* (2), 1340–1347.
- (16) Grenoble, Z.; Baldelli, S. Adsorption of the Cationic Surfactant Benzyltrimethylhexadecylammonium Chloride at the Silica-Water Interface and Metal Salt Effects on the Adsorption Kinetics. *J. Phys. Chem. B* **2013**, *117* (1), 259–272.
- (17) Zhang, H.; Ramakrishnan, T. S.; Nikolov, A.; Wasan, D. Enhanced Oil Displacement by Nanofluid's Structural Disjoining Pressure in Model Fractured Porous Media. *J. Colloid Interface Sci.* **2018**, *511*, 48–56.
- (18) Totland, C.; Lewis, R. T. Mechanism of Calcite Wettability Alteration by Alkyl Polyglucoside. *Colloids Surf., A* **2016**, *488*, 129–137.
- (19) Somasundaran, P.; Zhang, L. Adsorption of Surfactants on Minerals for Wettability Control in Improved Oil Recovery Processes. *J. Pet. Sci. Eng.* **2006**, *52* (1–4), 198–212.
- (20) Hirasaki, G.; Zhang, D. L. Surface Chemistry of Oil Recovery From Fractured, Oil-Wet, Carbonate Formations. *SPE J.* **2004**, *9* (02), 151–162.
- (21) Pal, N.; Kumar, S.; Bera, A.; Mandal, A. Phase Behaviour and Characterization of Microemulsion Stabilized by a Novel Synthesized Surfactant: Implications for Enhanced Oil Recovery. *Fuel* **2019**, *235*, 995–1009.
- (22) Jha, N. K.; Ali, M.; Iglauer, S.; Lebedev, M.; Roshan, H.; Barifani, A.; Sangwai, J. S.; Sarmadivaleh, M. Wettability Alteration of Quartz Surface by Low-Salinity Surfactant Nanofluids at High-Pressure and High-Temperature Conditions. *Energy Fuels* **2019**, *33*, 7062–7068.
- (23) Skauge, A.; Fotland, P. Effects of Temperature and Pressure on the Phase Behavior of Microemulsions. *SPE Reservoir Eng.* **1990**, *5*, 601.
- (24) Talebian, S. H.; Tan, I. M.; Masoudi, R.; Onur, M. Fluid-Fluid Interactions in a System of CO₂, Oil, Surfactant Solution, and Brine at High Pressures and Temperatures - A Malaysian Reservoir Case. *J. Pet. Sci. Eng.* **2014**, *124*, 313–322.
- (25) Yan, W.; Zhao, G. Y.; Chen, G. J.; Guo, T. M. Interfacial Tension of (Methane + Nitrogen) + Water and (Carbon Dioxide + Nitrogen) + Water Systems. *J. Chem. Eng. Data* **2001**, *46* (6), 1544–1548.
- (26) Chow, Y. T. F.; Maitland, G. C.; Trusler, J. P. M. Interfacial Tensions of the (CO₂ + N₂ + H₂O) System at Temperatures of (298 to 448) K and Pressures up to 40 MPa. *J. Chem. Thermodyn.* **2016**, *93*, 392–403.
- (27) Fathinasab, M.; Ayatollahi, S.; Hemmati-Sarapardeh, A. A Rigorous Approach to Predict Nitrogen-Crude Oil Minimum Miscibility Pressure of Pure and Nitrogen Mixtures. *Fluid Phase Equilib.* **2015**, *399*, 30–39.
- (28) Hemmati-Sarapardeh, A.; Mohagheghian, E. Modeling Interfacial Tension and Minimum Miscibility Pressure in Paraffin-Nitrogen Systems: Application to Gas Injection Processes. *Fuel* **2017**, *205*, 80–89.
- (29) Hemmati-Sarapardeh, A.; Ayatollahi, S.; Zolghadr, A.; Ghazanfari, M. H.; Masihi, M. Experimental Determination of Equilibrium Interfacial Tension for Nitrogen-Crude Oil during the Gas Injection Process: The Role of Temperature, Pressure, and Composition. *J. Chem. Eng. Data* **2014**, *59* (11), 3461–3469.
- (30) Hawthorne, S. B.; Miller, D. J.; Jin, L.; Gorecki, C. D. Rapid and Simple Capillary-Rise/Vanishing Interfacial Tension Method to Determine Crude Oil Minimum Miscibility Pressure: Pure and Mixed CO₂, Methane, and Ethane. *Energy Fuels* **2016**, *30* (8), 6365–6372.
- (31) Ratnakar, R. R.; Mantilla, C. A.; Dindoruk, B. Experimental Investigation of the Effects of Asphaltene Stability on Interfacial Behavior of Live-Reservoir-Fluid Systems. *SPE J.* **2019**, *24* (1), 21–31.
- (32) Ameli, F.; Hemmati-Sarapardeh, A.; Schaffie, M.; Husein, M. M.; Shamshirband, S. Modeling Interfacial Tension in N₂/n-Alkane Systems Using Corresponding State Theory: Application to Gas Injection Processes. *Fuel* **2018**, *222*, 779–791.
- (33) Wang, D.; Lin, M.; Dong, Z.; Li, L.; Jin, S.; Pan, D.; Yang, Z. Mechanism of High Stability of Water-in-Oil Emulsions at High Temperature. *Energy Fuels* **2016**, *30* (3), 1947–1957.
- (34) *Manual of Petroleum Measurement Standards. Chapter 11-Physical Properties Data. Section 1-Temperature and Pressure Volume Correction Factors for Generalized Crude Oils, Refined Products, and Lubricating Oils*; American Petroleum Institute: 2007.
- (35) GOST R 8.610-2004. *State System for Ensuring the Uniformity of Measurements. Density of Oil. The Tables for Recalculation*; Federal Agency for Technical Regulation and Metrology: 2004; p 15.
- (36) Wu, Y. High-Pressure and High-Temperature Density Measurements of n-Pentane, n-Octane, 2,2,4-Trimethylpentane, Cyclooctane, n-Decane, and Toluene. M.S. Thesis, Virginia Commonwealth University, 2010.
- (37) Wu, Y.; Bamgbade, B.; Liu, K.; McHugh, M. A.; Baled, H.; Enick, R. M.; Burgess, W. A.; Tapriyal, D.; Morreale, B. D. Experimental Measurements and Equation of State Modeling of Liquid Densities for Long-Chain n-Alkanes at Pressures to 265 MPa and Temperatures to 523K. *Fluid Phase Equilib.* **2011**, *311* (1), 17–24.
- (38) Abutaqiya, M. I. L.; Panuganti, S. R.; Vargas, F. M. Efficient Algorithm for the Prediction of Pressure-Volume-Temperature Properties of Crude Oils Using the Perturbed-Chain Statistical Associating Fluid Theory Equation of State. *Ind. Eng. Chem. Res.* **2017**, *56* (20), 6088–6102.
- (39) Yan, W.; Varzandeh, F.; Stenby, E. H. PVT Modeling of Reservoir Fluids Using PC-SAFT EoS and Soave-BWR EoS. *Fluid Phase Equilib.* **2015**, *386*, 96–124.
- (40) Hosseinfar, P.; Assareh, M.; Ghotbi, C. Developing a New Model for the Determination of Petroleum Fraction PC-SAFT Parameters to Model Reservoir Fluids. *Fluid Phase Equilib.* **2016**, *412*, 145–157.
- (41) Burgess, W. A.; Bamgbade, B. A.; Gamwo, I. K. Experimental and Predictive PC-SAFT Modeling Results for Density and Isothermal Compressibility for Two Crude Oil Samples at Elevated Temperatures and Pressures. *Fuel* **2018**, *218*, 385–395.
- (42) Liang, X.; Yan, W.; Thomsen, K.; Kontogeorgis, G. M. On Petroleum Fluid Characterization with the PC-SAFT Equation of State. *Fluid Phase Equilib.* **2014**, *375*, 254–268.
- (43) Cai, B. Y.; Yang, J. T.; Guo, T. M. Interfacial Tension of Hydrocarbon + Water/Brine Systems under High Pressure. *J. Chem. Eng. Data* **1996**, *41* (3), 493–496.
- (44) McCaffery, F. G. Measurement of Interfacial Tensions and Contact Angles At High Temperature and Pressure. *J. Can. Pet. Technol.* **1972**, *11* (3), 26–32.
- (45) Barati-Harooni, A.; Soleymanzadeh, A.; Tatar, A.; Najafi-Marghmaleki, A.; Samadi, S. J.; Yari, A.; Roushani, B.; Mohammadi, A. H. Experimental and Modeling Studies on the Effects of Temperature, Pressure and Brine Salinity on Interfacial Tension in Live Oil-Brine Systems. *J. Mol. Liq.* **2016**, *219*, 985–993.

(46) Pereira, L.; dos Santos, P. G.; Scheer, A. P.; Ndiaye, P. M.; Corazza, M. L. High Pressure Phase Equilibrium Measurements for Binary Systems CO₂ + 1-Pentanol and CO₂ + 1-Hexanol. *J. Supercrit. Fluids* **2014**, *88*, 38–45.

(47) Iglauer, S.; Wu, Y.; Shuler, P.; Tang, Y.; Goddard, W. A. Alkyl Polyglycoside Surfactant-Alcohol Cosolvent Formulations for Improved Oil Recovery. *Colloids Surf., A* **2009**, *339* (1–3), 48–59.

(48) Li, L.; Al-Muntasheri, G.; Liang, F. Nanomaterials-Enhanced High-Temperature Fracturing Liquids Prepared with Untreated Seawater. *SPE Annual Technical Conference and Exhibition*; Society of Petroleum Engineers: 2016. DOI: 10.2118/181283-MS.

(49) Ferreira, F. A.; Barbalho, T. C. S.; Araújo, I. R. S.; Oliveira, H. N. M.; Chiavone-Filho, O. Characterization, Pressure-Volume-Temperature Properties, and Phase Behavior of a Condensate and Crude oil. *Energy Fuels* **2018**, *32*, 5643–5649.

(50) Liu, R.; Du, D.-j.; Pu, W.; Zhang, J.; Fan, X.-b. Enhanced Oil Recovery Potential of Alkyl Alcohol Polyoxyethylene Ether Sulfonate Surfactants in High-Temperature and High Salinity Reservoirs. *Energy Fuels* **2018**, *32*, 12128–12140.

(51) Falbe, J. *Surfactants in Consumer Products*; Falbe, J., Ed.; Springer: Berlin, 1987; Chapter 4.1.

(52) Al-Ghamdi, A. M.; Nasr-el-din, H. Effect of Oilfield Chemicals on the Cloud Point of Nonionic Surfactants. *Colloids Surf., A* **1997**, *125*, 5–18.

(53) Sandersen, S. B.; Stenby, E. H.; von Solms, N. The Effect of Pressure on the Phase Behavior of Surfactant Systems: An Experimental Study. *Colloids Surf., A* **2012**, *415*, 159–166.

(54) Chow, Y. T. F.; Eriksen, D. K.; Galindo, G.; Haslam, A. J.; Jackson, G.; Maitland, G. C.; Trusler, J. P. M. Interfacial tensions of systems comprising water, carbon dioxide and diluent gases at high pressures: Experimental measurements and modelling with SAFT-VR Mie and square gradient theory. *Fluid Phase Equilib.* **2016**, *407*, 159–176.